
[View Journal Online](#)
[View Article Online](#)

Synthesis, crystal structure, DFT studies, and Hirshfeld surface analysis of *N,N'*-bis(3-quinolyl-methylene)diphenylethanedione dihydrazone

 Goutam Kumar Patra ^{1,*}, Amit Kumar Manna ¹ and Dinesh De ²
¹ Department of Chemistry, Faculty of Physical Sciences, Guru Ghasidas Vishwavidyalaya, Bilaspur (Chhattisgarh), 495009, India
goutam.patra@ggu.ac.in (G.K.P.), amitmanna51@gmail.com (A.K.M.)

² Department of Basic Science, Vishwavidyalaya Engineering College, Lakhanpur, CSVTU- Bhilai, Chhattisgarh-497116, India
d2chem@gmail.com (D.D.)

 * Corresponding author at: Department of Chemistry, Faculty of Physical Sciences, Guru Ghasidas Vishwavidyalaya, Bilaspur (Chhattisgarh), 495009, India.
 e-mail: goutam.patra@ggu.ac.in (G.K. Patra).

RESEARCH ARTICLE

ABSTRACT



doi 10.5155/eurjchem.12.4.394-400.2153

Received: 16 July 2021

Received in revised form: 20 August 2021

Accepted: 28 August 2021

Published online: 31 December 2021

Printed: 31 December 2021

KEYWORDS

 Dihydrazone
 Di-Schiff base
 Diphenylethanedione
 X-ray crystal structure
 Hirshfeld surface analysis
 Density functional theory (DFT)

The synthesis, characterization, and theoretical studies of a novel hydrazone, *N,N'*-bis-(3-quinolylmethylene)diphenylethanedione dihydrazone (1) has been reported. The molecular structure has been characterized by room-temperature single-crystal X-ray diffraction which reveals that two quinoline moieties are disposed nearly perpendicularly around the central C-C bond giving a 'L' shape of the molecule. This particular geometry gives rise to the hydrogen-bonded supramolecular rectangle of two self-complementary molecules. These supramolecular units are further assembled by π - π interaction. The Hirshfeld surface analysis of compound 1 shows that C...C, C...H, H...H, and N...H interactions of 13.1, 9.9, 52.3, and 7.4%, respectively, which exposed that the main intermolecular interactions were H...H intermolecular interactions. Crystal data for $C_{34}H_{24}N_6$: Triclinic, space group P-1 (no. 2), $a = 10.885(3)$ Å, $b = 11.134(3)$ Å, $c = 12.870(3)$ Å, $\alpha = 90.122(6)^\circ$, $\beta = 114.141(6)^\circ$, $\gamma = 110.277(5)^\circ$, $V = 1316.1(6)$ Å³, $Z = 2$, $T = 100(2)$ K, $\mu(\text{MoK}\alpha) = 0.080$ mm⁻¹, $D_{\text{calc}} = 1.304$ g/cm³, 7309 reflections measured ($3.518^\circ \leq 2\theta \leq 39.276^\circ$), 2318 unique ($R_{\text{int}} = 0.0527$, $R_{\text{sigma}} = 0.0565$) which were used in all calculations. The final R_1 was 0.0416 ($I > 2\sigma(I)$) and wR_2 was 0.1074 (all data).

Cite this: *Eur. J. Chem.* 2021, 12(4), 394-400Journal website: www.eurjchem.com

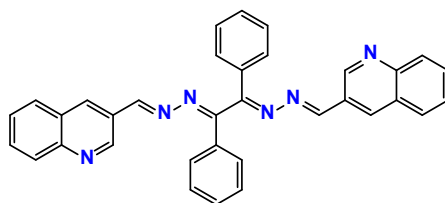
1. Introduction

Generally, Schiff bases provide suitable geometrical and electronic environments towards some selected main metal ions, thus responsible for stable host-guest interaction. The specific ion selectivity depends on the relative stability of the host-guest interaction, thus can be influenced by the cavity size, flexibility of the chelator, and hardness of the coordinating atom; whereas the optical response is due to influence of guest on the electronic environment of the chromo-fluorophore [1-6]. As the guest selective binding does not always produce a proper signal, thus tailor-made synthesis of a chemoreceptor with desired functionalities is necessary to achieve measurable signal through a change in emission and/or absorption upon coordination. After Jean-Marie Lehn's famous report of supramolecular chemistry [7], the chemistry of molecular assemblies and intermolecular noncovalent binding interactions, i.e. hydrogen bonding, ionic interactions and π - π stacking interactions have fascinated increasing attention in crystal engineering. In particular, hydrogen bonding π - π stacking interactions which is a powerful organizing force in designing various supramolecular and solid-state architectures [8-10], is extensively used not only for networking numerous organic and

organometallic compounds [11,12], but also for generating interesting supramolecular properties, such as electrical, optical and magnetic [13,14] properties. Quinoline groups, with effective sites for coordination to transition metal ions, have been used for the construction of supramolecular coordination compounds [15-18]. In addition, organic imino-quinolyl fragments have proved to be very useful in self-assembly through hydrogen bonding and π - π stacking, and the assembled products have relevance to biological systems [19]. Thus, imino-quinolyl ligand like *N,N'*-bis-(3-quinolylmethylene)diphenylethanedione dihydrazone has been designed and synthesized. Density functional theory (DFT) is a quantum mechanical (QM) method used in chemistry and physics to calculate the electronic structure of atoms, molecules and solids. It has been very popular in computational solid-state physics since the 1970s. In recent years, density functional theory has been a shooting star in theoretical modelling [20,21]. The development of better exchange-correlation functional made it possible to calculate many molecular properties with comparable accuracies to traditional correlated ab initio methods, with more favorable computational costs [22].

Table 1. Crystal data and Refinement parameters of compound **1**.

Empirical formula	C ₃₄ H ₂₄ N ₆
Formula weight	516.59
Temperature (K)	100(2)
Crystal system	Triclinic
Space group	<i>P</i> -1
<i>a</i> (Å)	10.885(3)
<i>b</i> (Å)	11.134(3)
<i>c</i> (Å)	12.870(3)
α (°)	90.122(6)
β (°)	114.141(6)
γ (°)	110.277(5)
Volume (Å ³)	1316.1(6)
<i>Z</i>	2
ρ_{calc} (g/cm ³)	1.304
μ (mm ⁻¹)	0.080
<i>F</i> (000)	540.0
Crystal size (mm ³)	0.24 × 0.20 × 0.19
Radiation	MoK α (λ = 0.71073)
2 θ range for data collection (°)	3.518 to 39.276
Index ranges	-10 ≤ <i>h</i> ≤ 10, -10 ≤ <i>k</i> ≤ 10, -12 ≤ <i>l</i> ≤ 12
Reflections collected	7309
Independent reflections	2318 [<i>R</i> _{int} = 0.0527, <i>R</i> _{sigma} = 0.0565]
Data/restraints/parameters	2318/0/457
Goodness-of-fit on <i>F</i> ²	1.000
Final <i>R</i> indexes [<i>I</i> ≥ 2 σ (<i>I</i>)]	<i>R</i> ₁ = 0.0416, <i>wR</i> ₂ = 0.0904
Final <i>R</i> indexes [all data]	<i>R</i> ₁ = 0.0747, <i>wR</i> ₂ = 0.1074
Largest diff. peak/hole (e Å ⁻³)	0.14/-0.20

**Scheme 1.** Chemical structure of compound **1**.

Literature survey revealed that the DFT has a great accuracy in reproducing the experimental values in terms of geometry, dipole moment, vibrational frequency, *etc.* [23]. Hirshfeld surface-based tools appear as a novel approach to this end [24,25].

2. Experimental

2.1. Materials and physical measurements

All chemicals used in this study were purchased from Aldrich Chemical Company, USA, and Acros Chemical Company, USA, and used without further purification unless otherwise mentioned. The melting point was determined by an electrothermal IA9000 series digital melting point apparatus and is uncorrected. Microanalyses were carried out using a Perkin-Elmer 2400II elemental analyzer. Infrared (IR) spectra and solution electronic spectra were recorded on Nicolet Magna IR (Series II) and Shimadzu UV-160A spectrophotometers, respectively. ¹H NMR spectra and electro-spray ionization mass (ESI-MS) measurements were made using a Bruker Advance 400 MHz and Finnigan LCQ Decap MAX mass spectrometer, respectively.

2.2. Synthesis of compound **1**

Diphenylethanedione dihydrazone (0.714 g, 3 mmol) was dissolved in anhydrous methanol (25 mL) and in the solution 3-quinoline carboxaldehyde (0.942 g, 6 mmol) was added. The reaction mixture was refluxed under dry atmosphere for about 6 h. Then it was slowly cooled to room temperature to obtain a yellow crystalline solid of compound **1**. The structure of the compound **1** has been confirmed by, mass spectrometry, ¹H and ¹³C NMR, IR and electronic spectroscopy.

N,N'-bis-(3-quinolylmethylene)diphenylethanedione dihydrazone (**1**) (Scheme 1): Color: Yellow. Yield: 80%. M.p.: 473 K. FT-IR (KBr, cm⁻¹): 3421 (wb), 3059 (w), 1612 (vs), 1569 (m), 1492 (m), 1448 (w), 1361 (w), 1315 (m), 1247 (m), 1172 (s), 968 (m), 785 (vs), 750 (s), 685 (vs), 464 (m). ¹H NMR (400 MHz, CDCl₃, δ , ppm): 9.16 (d, 2H, Ar-H), 8.67 (s, 2H, Ar-H), 8.27 (s, 2H, Ar-H), 8.16 (d, 2H, Ar-H), 7.92(d, 4H, Ar-H), 7.80 (s, 2H, -CH=N), 7.75 (t, 2H, Ar-H), 7.56 (t, 2H, Ar-H), 7.47 (m, 6H, Ar-H), 7.67 (t, 2H, Ar-H), 7.22-7.27 (m, 2H, Ar-H), 3.60 (t, 4H, -CH₂), 1.66 (q, 4H, -CH₂). ¹³C NMR (200 MHz, CDCl₃, δ , ppm): 166.53, 157.40, 148.58, 137.95, 134.03, 131.57, 131.51, 129.07, 128.64, 128.58, 128.03, 127.90, 127.69, 127.48. MS (EI, *m/z* (%)): 517.339 (LH⁺, 100). Anal. calcd. for C₃₄H₂₄N₆: C, 79.05; H, 4.68; N, 16.27. Found: C, 79.12; H, 4.59; N, 16.36%.

2.3. X-ray crystallography

X-ray single crystal data were collected using MoK α (λ = 0.7107 Å) radiation on a Bruker APEX II diffractometer equipped with CCD area detector. Data collection, data reduction, structure solution/refinement were carried out using the software package of SMART APEX [26]. The structures were solved by direct methods SHELXS-97 [27] and standard Fourier techniques, and refined on *F*² using full matrix least squares procedures SHELXL-97 using the SHELX-97 package incorporated in WinGX [28]. Whenever possible, the hydrogen atoms were located on a difference Fourier map and refined. In other cases, the hydrogen atoms were geometrically fixed. The crystallographic details of compound **1** are summarized in Table 1, selected bond lengths and angles of **1** is listed in Tables 2 and 3 and selected hydrogen bonding parameters of compound **1** is shown in Table 4.

Table 2. Bond distances for compound 1.

Atom	Atom	Length (Å)	Atom	Atom	Length (Å)
C2	C3	1.363(5)	C14	C22	1.451(5)
C2	C1	1.424(5)	C16	C17	1.412(5)
C2	C10	1.446(5)	C16	C15	1.414(5)
C3	C4	1.417(5)	C16	C21	1.416(5)
C4	C5	1.418(5)	C17	C18	1.411(5)
C4	C9	1.418(5)	C20	C21	1.368(5)
C5	C6	1.360(6)	C20	C19	1.395(6)
C7	C8	1.361(6)	C18	C19	1.364(6)
C7	C6	1.393(6)	C22	N5	1.276(4)
C8	C9	1.394(5)	N6	N5	1.410(4)
C1	N1	1.323(5)	N6	C34	1.291(4)
C9	N1	1.380(5)	C23	C24	1.392(5)
C10	N2	1.284(4)	C23	C28	1.383(5)
N2	N3	1.422(4)	C23	C34	1.486(5)
N3	C11	1.290(4)	C24	C25	1.389(6)
C12	C11	1.473(5)	C28	C27	1.382(6)
C12	C29	1.379(5)	C27	C26	1.369(6)
C12	C33	1.393(5)	C26	C25	1.371(6)
C11	C34	1.510(5)	C29	C30	1.379(5)
N4	C17	1.374(5)	C33	C32	1.384(5)
N4	C13	1.325(5)	C31	C32	1.375(5)
C14	C13	1.412(5)	C31	C30	1.367(5)

Table 3. Bond angles for compound 1.

Atom	Atom	Atom	Angle (°)	Atom	Atom	Atom	Angle (°)
C3	C2	C1	117.6(4)	C17	C16	C21	118.9(4)
C3	C2	C10	120.6(4)	C15	C16	C21	123.1(4)
C1	C2	C10	121.8(4)	N4	C17	C16	122.8(4)
C2	C3	C4	120.8(4)	N4	C17	C18	117.9(4)
C3	C4	C5	123.4(4)	C16	C17	C18	119.3(4)
C3	C4	C9	117.4(4)	N4	C13	C14	125.1(4)
C5	C4	C9	119.2(4)	C14	C15	C16	119.6(4)
C6	C5	C4	120.0(5)	C21	C20	C19	121.0(5)
C8	C7	C6	121.6(5)	C20	C21	C16	120.0(5)
C7	C8	C9	120.0(5)	C19	C18	C17	120.4(5)
N1	C1	C2	124.3(4)	C18	C19	C20	120.3(5)
C5	C6	C7	120.0(5)	N5	C22	C14	121.3(4)
C8	C9	C4	119.1(4)	C34	N6	N5	111.3(3)
N1	C9	C4	122.0(4)	C22	N5	N6	111.9(3)
N1	C9	C8	118.9(4)	C24	C23	C34	121.1(4)
C1	N1	C9	117.9(4)	C28	C23	C24	118.6(4)
N2	C10	C2	121.8(4)	C28	C23	C34	120.2(4)
C10	N2	N3	111.1(3)	C25	C24	C23	120.7(5)
C11	N3	N2	112.6(3)	C23	C28	C27	120.5(5)
C29	C12	C11	121.6(4)	C26	C27	C28	120.2(5)
C29	C12	C33	118.2(4)	C27	C26	C25	120.6(5)
C33	C12	C11	120.2(4)	C26	C25	C24	119.4(5)
N3	C11	C12	119.4(4)	C30	C29	C12	121.2(5)
N3	C11	C34	123.6(3)	C32	C33	C12	120.1(4)
C12	C11	C34	116.9(4)	C30	C31	C32	119.4(5)
C13	N4	C17	116.7(4)	C31	C32	C33	120.7(5)
C13	C14	C22	119.6(4)	C31	C30	C29	120.4(5)
C15	C14	C13	117.8(4)	N6	C34	C11	122.8(3)
C15	C14	C22	122.6(4)	N6	C34	C23	118.3(3)
C17	C16	C15	117.9(4)	C23	C34	C11	118.5(4)

Table 4. Hydrogen bonding parameters for compound 1.

D-H...A	D-H (Å)	H...A (Å)	D...A (Å)	∠D-H...A (°)	Symmetry
C13-H5...N1	0.99(4)	2.60(4)	3.587(7)	170(3)	1-x, 2-y, 2-z

2.4. Theoretical calculations

Gaussian 09 program [29] has been used for quantum chemical calculations. The possible ground state structures have been optimized with density functional theory (DFT) at B3LYP/6-311G**. GaussView 5 program [30] was used for the visualization of the studied systems.

2.5. Hirshfeld surfaces calculation

Hirshfeld surface analysis helps as a powerful set-up for obtaining additional insight into the intermolecular interaction of molecular crystals. The size and shape of Hirshfeld surface allows the qualitative and quantitative study and imaging of intermolecular close contacts in molecular crystals [31]. The Hirshfeld surface enclosing a molecule is defined by a set of

points in 3D space where the contribution to the electron density from the molecule of interest is equal to the contribution from all other molecules.

Molecular Hirshfeld surfaces are constructed based on electron distribution calculated as the sum of spherical atom electron densities [32]. Thus, an iso-surface is obtained, and for each point of the iso-surface two distances can be defined: d_e , the distance from the point to the nearest atom outside to the surface, and d_i , the distance to the nearest atom inside to the surface. Moreover, the identification of the regions of particular importance to intermolecular interactions is obtained by mapping normalized contact distance (d_{norm}), expressed as: $d_{norm} = (d_i - r_i^{vdw}) / r_i^{vdw} + (d_e - r_e^{vdw}) / r_e^{vdw}$; where r_i^{vdw} and r_e^{vdw} are the van der Waals radii of the atoms [33]. The value of d_{norm} is negative or positive when intermolecular contacts are shorter or longer than r^{vdw} , respectively.

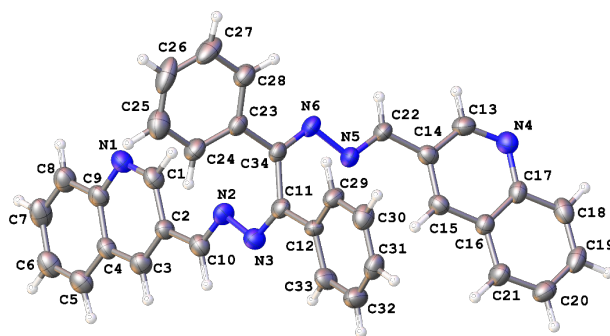


Figure 1. The ORTEP diagram (30% ellipsoidal probability) of compound **1** with atom numbering scheme.

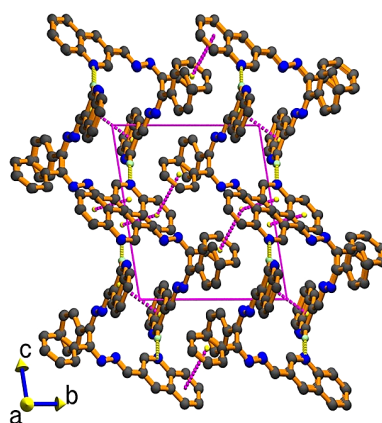


Figure 2. The self-assembled molecular rectangle through hydrogen bonding in compound **1**.

Graphical plots of the molecular Hirshfeld surfaces mapped with d_{norm} employ the red-white-blue color scheme, where red color indicates the shorter intermolecular contacts, white color show the contacts around the r^{vdw} separation, and blue color is used to indicate the longer contact distances. Because of the symmetry between d_e and d_i in the expression for d_{norm} , where two Hirshfeld surfaces touch, both will display a red spot identical in color intensity as well as size and shape [34]. The combination of d_e and d_i in the form of a 2D fingerprint plot provides summary of intermolecular contacts in the crystal and are in complement to the Hirshfeld surfaces. Such plots provide information about the intermolecular interactions in the immediate environment of each molecule in the asymmetric unit. Moreover, the close contacts between particular atom types can be highlighted in so-called resolved fingerprint plots, which allow the facile assignment of an intermolecular contact to a certain type of interaction and quantitatively summarize the nature and type of intermolecular contacts. Two additional colored properties (shape index and curvedness) based on the local curvature of the surface can also be specified [35]. The Hirshfeld surfaces are mapped with d_{norm} , shape-index, curvedness and 2D fingerprint plots (full and resolved) presented in this paper were generated using Crystal-Explorer 3.1 [36].

3. Results and discussion

3.1. Synthesis and structure

The compound **1** was synthesized in good yield and as yellow solid by condensing diphenylethanedione dihydrazone and quinoline 3-carboxaldehyde in 1:2 molar ratio in anhydrous methanol [37,38]. The compound **1** under study shows characteristic peak at 1612 cm^{-1} is assigned to the imine

(C=N) stretching frequencies. The ^1H NMR spectra of the compound **1** in CDCl_3 showed a singlet at δ 7.80 ppm due to HC=N proton, other aryl protons resonates in between δ 9.16 to 7.47 ppm. In the ^{13}C NMR spectra the $-\text{C}=\text{N}$ carbon appears at δ 166.53 ppm and the other aryl carbons resonate between δ 157.50 to 127.48 ppm (expected region). Compound **1** crystallizes in the triclinic space group $P-1$ and the asymmetric unit contains a single molecule of compound **1** (Scheme 1). Due to the steric crowding between the two phenyl groups substituted on the central C-C bond in compound **1** the $\text{N}=\text{C}-\text{C}=\text{N}$ and $\text{C}(\text{Ph})-\text{C}-\text{C}(\text{Ph})$ torsion angles about this bond are -102.25 and -93.55° , respectively.

The molecule consists of two identical linear parts connected covalently by a C-C bond at the C11 and C34 carbon (Figure 1). Each segment of the molecule is linear and is nearly orthogonally disposed with respect to each other.

This gives rise to the 'L' shape of the molecule with two phenyl groups acting as small appendages. Each of the linear segments of the molecule consists of a phenyl and a quinoline group on either side of the central azo group. The molecule is rigid and the plane of the quinoline groups on both branches is perpendicular to each other.

The 'L' shape of the molecule is self-complementary for hydrogen bonding. The crystal structure analysis reveals a hydrogen bonded supramolecular rectangle (Figure 2). The quinoline nitrogen atom N1 acts as an acceptor for the hydrogen attached to the C13 carbon atom adjacent to the N atom. The hydrogen bonding parameters are given in Table 4.

The size and aromatic nature of the quinoline fragment reveals a high propensity for strong dispersive interactions between the flat molecular surfaces of these rings in the condensed solid phase. This spatial as well as enthalpic element is well expressed in the crystal packing arrangement of compound **1**.

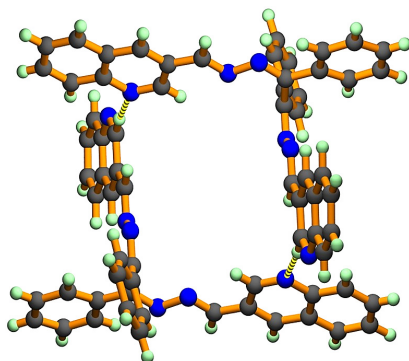


Figure 3. The π - π stacking of hydrogen bonded molecular rectangles in compound 1.

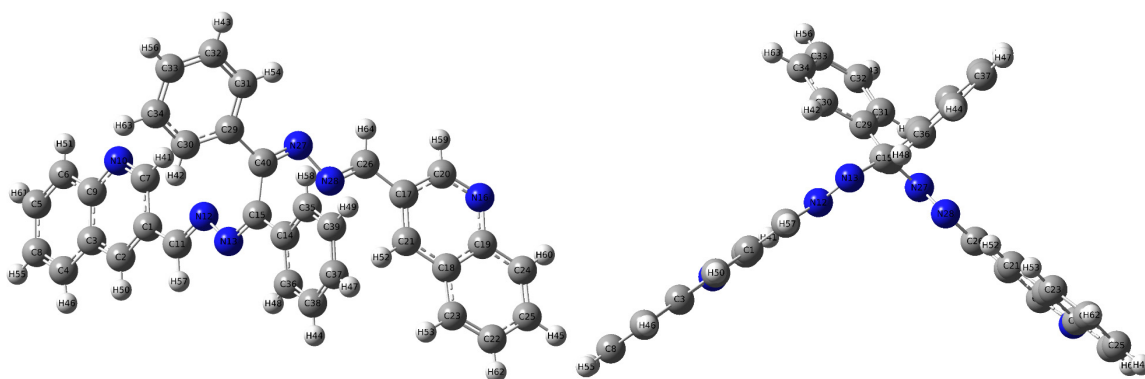


Figure 4. Optimized molecular structure of compound 1.

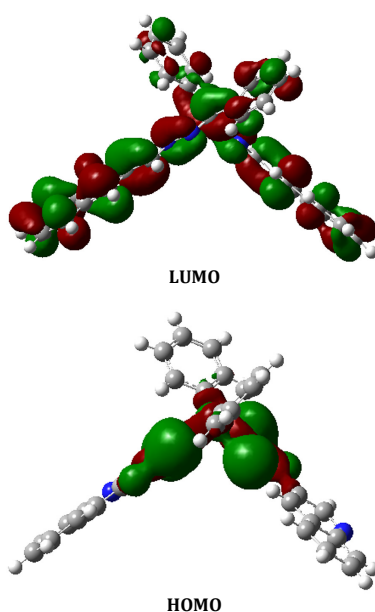


Figure 5. Surface plots of HOMO and LUMO of the ligand 1.

The π - π stacking interaction between the aromatic 3-quinoline rings of neighboring molecules has been observed in the crystals of compound 1. Face-to-face overlap between the phenyl substituent of one species and the quinoline substituent of another species provides an additional stabilizing contribution. Hydrogen bonded molecular rectangles are thus joined at their corners by π - π interaction (Figure 3). In a unit cell four such rectangles are there, center of each is positioned at the cell corners.

3.2. Theoretical investigations

The optimized bond lengths and angles for the compound 1 is well replicated with the experimental single crystal X-ray diffraction structure data. The optimized structure of compound 1 has been shown in Figure 4. The surface plots of HOMO and LUMO of compound 1 have been depicted in Figure 5.

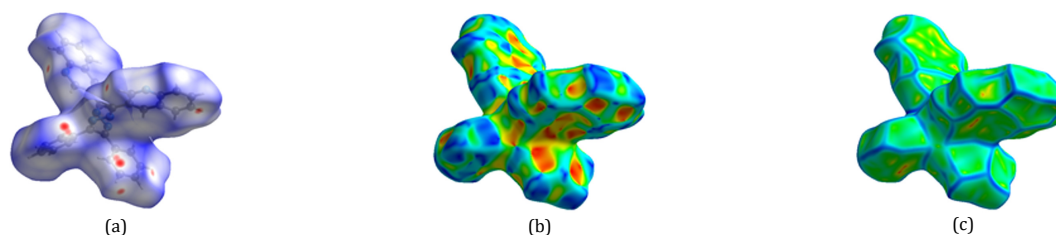


Figure 6. Hirshfeld surfaces of compound **1**: (a) 3D d_{norm} surface, (b) shape index, and (c) curvedness.

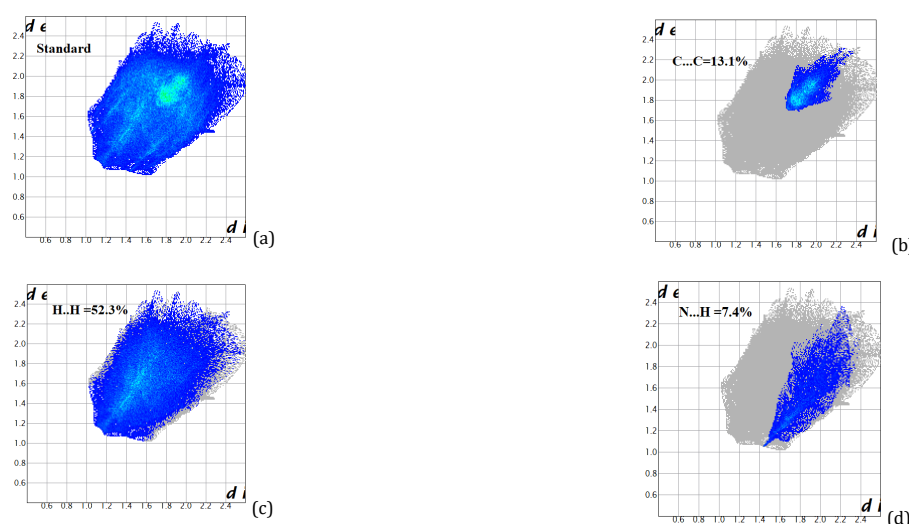


Figure 7. 2D Fingerprint plots of compound **1**, (a) standard full, (b) resolved into C...C, (c) resolved into H...H, and (d) N...H contacts, showing the percentages of contacts contributing to the total Hirshfeld surface area of the molecule.

3.3. Molecular Hirshfeld surfaces

The Hirshfeld surface is a suitable tool for describing the surface characteristics of molecules. The molecular Hirshfeld surface of compound **1** was generated using a standard (high) surface resolution with the 3D d_{norm} surfaces mapped over a fixed color scale of -0.22 (red) to 1.4 Å (blue). The shape index mapped in the color range of -0.99 to 1.0, and the curvedness was in the range of -4.0 to 0.4. The surfaces were shown to be transparent to allow visualization of the molecular moiety in a similar orientation for all of the structures around which they were calculated. The molecular Hirshfeld surface (d_{norm} , Shape index and Curvedness) of compound **1** has been shown in Figure 6.

The Hirshfeld surface analysis of compound **1** shows that C...C, H...H, C...H, and N...H interactions of 13.1, 52.3, 9.9 and 7.4%, respectively, which revealed that the main intermolecular interactions were H...H intermolecular interactions. Both the C...C and C...H interactions were represented almost same area by a small area in the right side of the top in the 2D fingerprint map, whereas the H...H interactions were represented by the largest in the fingerprint plot (Figure 7) and thus had the most significant contribution to the total Hirshfeld surfaces (52.3%).

3.4. Molecular electrostatic potential (MEP)

The potential increases in the order red < yellow < green < blue < pink < white. Red and yellow represent the regions of most negative electrostatic potential which is related to electrophilic reactivity, white represents the region of most positive electrostatic potential which is related to nucleophilic reactivity and blue represents the region of zero potential.

Molecular electrostatic potential (MEP) of compound **1** has been shown in Figure 8.

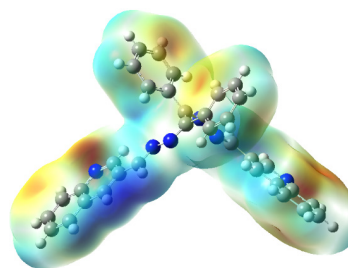


Figure 8. Molecular electrostatic potential of compound **1**.

4. Conclusion

In conclusion, we have synthesized a polydentate imino quinolyl ligand, *N,N'*-bis-(3-quinolylmethylene)diphenylethane dione dihydrazone and determined its single crystal X-ray structure at room temperature. Interestingly this molecule is predisposed for supramolecular rectangles due to its 'L' shaped geometry as well as self-complementarity in hydrogen bonding. Generation of molecules or supramolecular architecture of different well-known geometries such as triangles, square, pentagon- in general n -gon is a challenging task in crystal engineering. In this respect, the molecule reported here shows how the design principle, especially 'L' shape and suitable positioning of acceptor and donors can give rise to targeted geometry. The Hirshfeld surface analysis of compound **1** shows that C...C, C...H, H...H, and N...H interactions of 13.1, 9.9, 52.3, and 7.4%, respectively, which exposed that the main intermolecular interactions were H...H intermolecular interactions.

Acknowledgements

Goutam Kumar Patra would like to thank the Department of Science and Technology (SR/FST/CSI-264/2014 and EMR/2017/0001789) and Department of Biotechnology, Government of India, New Delhi for financial support. Amit Kumar Manna thanks the Council for Scientific and Industrial Research, Government of India, for financial support in the form of research fellowships.

Supporting information

CCDC-805764 contains the supplementary crystallographic data for this paper. These data can be obtained free of charge via <https://www.ccdc.cam.ac.uk/structures/>, or by e-mailing data_request@ccdc.cam.ac.uk, or by contacting The Cambridge Crystallographic Data Centre, 12 Union Road, Cambridge CB2 1EZ, UK; fax: +44(0)1223-336033.

Disclosure statement

Conflict of interests: The authors declare that they have no conflict of interest.

Ethical approval: All ethical guidelines have been adhered.

Sample availability: Sample of compound **1** is available from the author.

CRedit authorship contribution statement

Conceptualization: Goutam Kumar Patra; Methodology: Goutam Kumar Patra; Software: Dinesh De; Validation: Amit Kumar Manna; Formal Analysis: Amit Kumar Manna; Investigation: Amit Kumar Manna; Resources: Goutam Kumar Patra; Data Curation: Dinesh De; Writing - Original Draft: Goutam Kumar Patra; Writing - Review and Editing: Goutam Kumar Patra; Visualization: Amit Kumar Manna; Funding acquisition: Goutam Kumar Patra; Supervision: Goutam Kumar Patra; Project Administration: Goutam Kumar Patra.

ORCID

Amit Kumar Manna

 <https://orcid.org/0000-0002-9605-2168>

Dinesh De

 <https://orcid.org/0000-0001-7850-8718>

Goutam Kumar Patra

 <https://orcid.org/0000-0003-3151-0284>

References

- Janiak, C.; Scharmann, T. G. *Polyhedron* **2003**, *22* (8), 1123–1133.
- Janiak, C. *Dalton Trans.* **2003**, *14*, 2781–2804.
- Rout, K.; Manna, A. K.; Sahu, M.; Mondal, J.; Singh, S. K.; Patra, G. K. *RSC Adv.* **2019**, *9* (44), 25919–25931.
- Pal, S.; Pal, S. *Polyhedron* **2003**, *22* (6), 867–873.
- Patra, G. K.; Pal, P. K.; Mondal, J.; Ghorai, A.; Mukherjee, A.; Saha, R.; Fun, H.-K. *Inorganica Chim. Acta* **2016**, *447*, 77–86.
- Mondal, J.; Mukherjee, A.; Patra, G. K. *Inorganica Chim. Acta* **2017**, *463*, 44–53.
- Manna, A. K.; Mondal, J.; Chandra, R.; Rout, K.; Patra, G. K. *J. Photochem. Photobiol. A Chem.* **2018**, *356*, 477–488.
- Lehn, J.-M. *Angew. Chem. Int. Ed. Engl.* **1988**, *27* (1), 89–112.
- Subramanian, S.; Zaworotko, M. J. *Coord. Chem. Rev.* **1994**, *137*, 357–401.
- Biradha, K.; Fujita, M. *Angew. Chem. Int. Ed. Engl.* **2002**, *41* (18), 3392–3395.
- Braga, D.; Bazzi, C.; Maini, L.; Grepioni, F. *CrystEngComm* **1999**, *1* (5), 15–20.
- Desiraju, G. R. The Supramolecular Synthon in Crystal Engineering. In *Stimulating Concepts in Chemistry*; Wiley-VCH Verlag GmbH & Co. KGaA: Weinheim, FRG, 2005; pp 293–306.
- Fernandes, J. D.; Maximino M. D.; Braunger, M. L.; Pereira, M. S.; Olivati, C. A.; Constantino, C. J. L.; Alessio, P. *Phys. Chem. Chem. Phys.* **2020**, *22*, 13554–13562.
- Zaworotko, M. J. *Angew. Chem. Int. Ed. Engl.* **2000**, *39* (17), 3052–3054.
- Baratta, W.; Ballico, M.; Baldino, S.; Chelucci, G.; Herdtweck, E.; Siega, K.; Magnolia, S.; Rigo, P. *Chemistry* **2008**, *14* (30), 9148–9160.
- Létard, J.-F.; Guionneau, P.; Rabardel, L.; Howard, J. A. K.; Goeta, A. E.; Chasseau, D.; Kahn, O. *Inorg. Chem.* **1998**, *37* (17), 4432–4441.
- Arun, V.; Robinson, P. P.; Manju, S.; Leeju, P.; Varsha, G.; Digna, V.; Yusuff, K. K. M. *Dyes Pigm.* **2009**, *82* (3), 268–275.
- Machura, B.; Kruszynski, R. *Polyhedron* **2007**, *26* (14), 3686–3694.
- Maspoch, D.; Ruiz-Molina, D.; Veciana, J. J. *Mater. Chem.* **2004**, *14* (18), 2713–2723.
- Rajendran, V.; Shyamala, D.; Loganayaki, M.; Ramasamy, P. *Mater. Lett.* **2007**, *61* (16), 3477–3479.
- Jeyakumari, A. P.; Manivannan, S.; Dhanuskodi, S. *Spectrochim. Acta A Mol. Biomol. Spectrosc.* **2007**, *67* (1), 83–86.
- De Proft, F.; Geerlings, P. *Chem. Rev.* **2001**, *101* (5), 1451–1464.
- Tanak, H. *Int. J. Quantum Chem.* **2012**, *112* (11), 2392–2402.
- Moggach, S. A.; Parsons, S.; Wood, P. A. *Crystallogr. Rev.* **2008**, *14* (2), 143–184.
- Parkin, A.; Barr, G.; Dong, W.; Gilmore, C. J.; Jayatilaka, D.; McKinnon, J. J.; Spackman, M. A.; Wilson, C. C. *CrystEngComm* **2007**, *9* (8), 648–652.
- Boehr, D. D.; Farley, A. R.; Wright, G. D.; Cox, J. R. *Chem. Biol.* **2002**, *9* (11), 1209–1217.
- Bruker (2008). SAINT, SMART. Bruker AXS Inc., Madison, Wisconsin, USA.
- Sheldrick, G. M. *Acta Crystallogr. A* **2008**, *64* (Pt 1), 112–122.
- Farrugia, L. J. *J. Appl. Cryst.* **2012**, *45*, 849–854.
- Frisch, M. J.; Trucks, G. W.; Schlegel, H. B.; Scuseria, G. E.; Robb, M. A.; Cheeseman, J. R.; Scalmani, G.; Barone, V.; Mennucci, B.; Petersson, G. A.; Nakatsuji, H.; Caricato, M.; Li, X.; Hratchian, H. P.; Izmaylov, A. F.; Bloino, J.; Zheng, G.; Sonnenberg, J. L.; Hada, M.; Ehara, M.; Toyota, K.; Fukuda, R.; Hasegawa, J.; Ishida, M.; Nakajima, T.; Honda, Y.; Kitao, O.; Nakai, H.; Vreven, T.; Montgomery, J. A.; Peralta, J. E.; Ogliaro, F.; Bearpark, M.; Heyd, J. J.; Brothers, E.; Kudin, K. N.; Staroverov, V. N.; Kobayashi, R.; Normand, J.; Raghavachari, K.; Rendell, A.; Burant, J. C.; Iyengar, S. S.; Tomasi, J.; Cossi, M.; Rega, N.; Millam, J. M.; Klene, M.; Knox, J. E.; Cross, J. B.; Bakken, V.; Adamo, C.; Jaramillo, J.; Gomperts, R.; Stratmann, R. E.; Yazyev, O.; A. J. Austin, A. J.; Cammi, R.; Pomelli, C.; Ochterski, J. W.; Martin, R. L.; Morokuma, K.; Zakrzewski, V. G.; Voth, G. A.; Salvador, P.; Dannenberg, J. J.; Dapprich, S.; Daniels, A. D.; Farkas, O.; Foresman, J. B.; Ortiz, J. V.; Cioslowski, J.; Fox, D. J. Gaussian, Inc., Gaussian 09, Revision A.02, Wallingford CT, 2009.
- Norret, M.; Makha, M.; Sobolev, A. N.; Raston, C. L. *New J. Chem.* **2008**, *32* (5), 808–812.
- Meng, X. X. Applications of Hirshfeld surfaces to ionic and mineral crystals, Ph.D. Thesis, University of New England, 2004.
- Pendas, A. M.; Luaña, V.; Pueyo, L.; Francisco, E.; Mori-Sanchez, P. J. *Chem. Phys.* **2002**, *117* (3), 1017–1023.
- Desiraju, G. R. *Angew. Chem. Int. Ed. Engl.* **2007**, *46* (44), 8342–8356.
- Schmidt, G. M. J. *Pure Appl. Chem.* **1971**, *27* (4), 647–678.
- Wolff, S. K.; Grimwood, D. J.; McKinnon, J. J.; Turner, M. J.; Jayatilaka, D.; Spackman, M. A. CrystalExplorer (Version 3.1); University of Western Australia, 2012.
- Patra, G. K.; Goldberg, I. *Cryst. Growth Des.* **2003**, *3* (3), 321–329.
- Busch, D. H.; Bailar, J. C., Jr. *J. Am. Chem. Soc.* **1956**, *78* (6), 1137–1142.



Copyright © 2021 by Authors. This work is published and licensed by Atlanta Publishing House LLC, Atlanta, GA, USA. The full terms of this license are available at <http://www.eurjchem.com/index.php/eurjchem/pages/view/terms> and incorporate the Creative Commons Attribution-Non Commercial (CC BY NC) (International, v4.0) License (<http://creativecommons.org/licenses/by-nc/4.0>). By accessing the work, you hereby accept the Terms. This is an open access article distributed under the terms and conditions of the CC BY NC License, which permits unrestricted non-commercial use, distribution, and reproduction in any medium, provided the original work is properly cited without any further permission from Atlanta Publishing House LLC (European Journal of Chemistry). No use, distribution or reproduction is permitted which does not comply with these terms. Permissions for commercial use of this work beyond the scope of the License (<http://www.eurjchem.com/index.php/eurjchem/pages/view/terms>) are administered by Atlanta Publishing House LLC (European Journal of Chemistry).